J|A|C|S ARTICLES

Published on Web 04/30/2009

Photogelling Colloidal Dispersions Based on Light-Activated Assembly of Nanoparticles

Kunshan Sun,[†] Rakesh Kumar,[†] Daniel E. Falvey,[‡] and Srinivasa R. Raghavan*,[†]

Department of Chemical and Biomolecular Engineering and Department of Chemistry and Biochemistry, University of Maryland, College Park, Maryland 20742-2111

Received February 10, 2009; E-mail: sraghava@eng.umd.edu

Abstract: Photorheological (PR) fluids, i.e., fluids whose rheology can be tuned by light, have been a recent focus for our laboratory. We are interested in low-cost approaches to PR fluids using molecules or materials that are readily available. Toward this end, we report a new concept for such fluids based on light-activated assembly of nanoparticles into a physical network (gel). Our system consists of disk-like nanoparticles of laponite along with a surfactant stabilizer (Pluronic F127) and the photoacid generator (PAG), diphenyliodonium-2-carboxylate monohydrate. Initially, the nanoparticles are sterically stabilized by the surfactant, and the result is a stable, low-viscosity dispersion. Upon UV irradiation, the PAG gets photolyzed, lowering the pH by ~3 units. In turn, the stabilizing surfactant is displaced from the negatively charged faces of the nanoparticle disks while the edges of the disks become positively charged. The particles are thereby induced to assemble into a three-dimensional "house-of-cards" network that extends through the sample volume. The net result is a light-induced *sol to gel transition*, i.e., from a low, water-like viscosity to an *infinite* viscosity and yield stress. The yield stress of the photogel is sufficiently high to support the weight of small objects. The gel can be converted back to a sol by increasing either the pH or the surfactant content.

1. Introduction

Numerous research groups[1−13] have been interested in creating fluids whose rheological properties, such as viscosity, can be tuned by irradiation with light (for reviews, see refs 2−5). Such *photorheological* (PR) fluids[1,12] could be particularly attractive for creating microvalves or flow sensors within microfluidic systems. Indeed, compared to other external stimuli such as heat or magnetic fields, light does offer distinct advantages in microscale applications, notably, in its ability to be directed at a precise spot with micron-level resolution. For PR fluids to be used widely, researchers need to be able to create them at will, preferably from inexpensive and commercially available components. However, most of the PR systems developed to date have been based on complex organic molecules, such as photoresponsive surfactants,[3,6,7] polymers,[5,8,9] or gelators,[4,10,11] most of which are not commercially available and whose synthesis demands considerable skill in organic chemistry. There is a need for simpler approaches to making PR fluids, and this has been the focus of our work.

Recently, we have demonstrated two PR fluids, a photothinning one[12] and a photogelling one,[13] both of which are based on simple, widely available molecules. Both fluids employed the photoisomerizable organic molecule, *trans-ortho*-methoxycinnamic acid (OMCA). The photothinning fluid combined OMCA with a conventional cationic surfactant.[12] In this case, UV irradiation of the fluid caused a substantial decrease in viscosity (factors of 1000 to 10 000). The photogelling fluid combined OMCA with a zwitterionic surfactant, and in this case, the fluid viscosity increased dramatically upon UV irradiation.[13] The mechanisms for the photorheological effects in both systems involved changes in the length of cylindrical ("wormlike") micelles. When the micelles were short, the viscosity was low; conversely, long micellar chains entangled with each other to give a high viscosity. The micelle length, in turn, was modulated by the binding tendency of the OMCA isomer (*trans* vs *cis*). In both of the above systems, the light-induced viscosity change was not reversible by irradiation with a different wavelength of light, but it was reversible by changing the system composition. Despite this limitation, our studies showed that significant light-induced rheological changes are indeed possible in very simple systems.

[†] Department of Chemical and Biomolecular Engineering.
[‡] Department of Chemistry and Biochemistry.

(1) Wolff, T.; Emming, C. S.; Suck, T. A.; Von Bunau, G. *J. Phys. Chem.* **1989**, *93*, 4894–4898.
(2) Wolff, T.; Klaussner, B. *Adv. Colloid Interface Sci.* **1995**, *59*, 31–94.
(3) Eastoe, J.; Vesperinas, A. *Soft Matter* **2005**, *1*, 338–347.
(4) Paulusse, J. M. J.; Sijbesma, R. P. *Angew. Chem., Int. Ed.* **2006**, *45*, 2334–2337.
(5) Yager, K. G.; Barrett, C. J. *J. Photochem. Photobiol., A* **2006**, *182*, 250–261.
(6) Lee, C. T.; Smith, K. A.; Hatton, T. A. *Macromolecules* **2004**, *37*, 5397–5405.
(7) Sakai, H.; Orihara, Y.; Kodashima, H.; Matsumura, A.; Ohkubo, T.; Tsuchiya, K.; Abe, M. *J. Am. Chem. Soc.* **2005**, *127*, 13454–13455.
(8) Moniruzzaman, M.; Sabey, C. J.; Fernando, G. F. *Polymer* **2007**, *48*, 255–263.
(9) Pouliquen, G.; Amiel, C.; Tribet, C. *J. Phys. Chem. B* **2007**, *111*, 5587–5595.
(10) Yagai, S.; Nakajima, T.; Kishikawa, K.; Kohmoto, S.; Karatsu, T.; Kitamura, A. *J. Am. Chem. Soc.* **2005**, *127*, 11134–11139.
(11) Matsumoto, S.; Yamaguchi, S.; Ueno, S.; Komatsu, H.; Ikeda, M.; Ishizuka, K.; Iko, Y.; Tabata, K. V.; Aoki, H.; Ito, S.; Noji, H.; Hamachi, I. *Chem.—Eur. J.* **2008**, *14*, 3977–3986.
(12) Ketner, A. M.; Kumar, R.; Davies, T. S.; Elder, P. W.; Raghavan, S. R. *J. Am. Chem. Soc.* **2007**, *129*, 1553–1559.
(13) Kumar, R.; Raghavan, S. R. *Soft Matter* **2009**, *5*, 797–803.

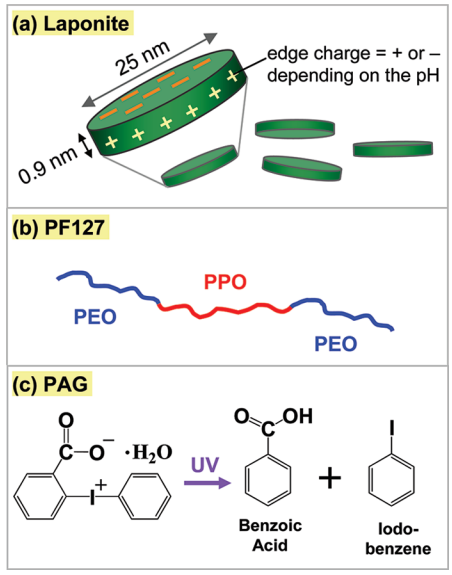

Figure 1. The three key components of the photorheological (PR) fluids described in this paper. (a) Laponite nanoparticles; (b) the triblock copolymer, Pluronic F127 (PF127); and (c) the photoacid generator (PAG), diphenyliodonium-2-carboxylate monohydrate. Upon UV irradiation, the PAG gets photolyzed into benzoic acid and iodobenzene.

In this paper, we report a new class of PR fluids based on an entirely different concept compared to the one discussed above. The key ingredient in our present fluids are *nanoscale particles* of the synthetic clay, laponite (Figure 1a).[14−17] These particles are initially dispersed in water as individual, unconnected disks, thus forming a low-viscosity fluid. Upon irradiation with UV light, the particles are induced to assemble into a three-dimensional network (called a "house-of-cards" structure in the literature[14−17]). The resulting aqueous gel has an infinite viscosity and a yield stress. In effect, our system shows a light-induced sol−gel transition, with the gel being held by physical (electrostatic) bonds. The gel can be converted back to a sol by changing the pH, but not by irradiation with a different wavelength of light.

How does this work? In addition to the laponite, the fluids have two other components (Figure 1b, 1c): the nonionic surfactant, Pluronic F127 (PF127), and the photoacid generator, diphenyliodonium-2-carboxylate monohydrate (abbreviated as "PAG" henceforth). Each of these components has a key role to play. PF127 is known to be a stabilizing surfactant for laponite: it adsorbs on the particle faces and provides steric stabilization.[18] Photoacid generators (PAGs) are commercially available organic molecules that have a key property: when irradiated with UV light, the molecules are photolyzed, with one of their photoproducts being an acidic moiety.[19−22] As a result, the solution pH drops by an amount proportional to the PAG concentration (this can be as much as 3 pH units). While a variety of PAGs are available, the PAG chosen here has a relatively high solubility in water.[21,23] Briefly, the mechanism behind the photogelling is as follows: initially, in the sol state, the particles are covered by PF127. Upon UV irradiation, the pH drops and, in turn, the particle edges become positively charged.[15,16] At the same time, the PF127 desorbs from the particles and forms micelles in solution. The positively charged particle edges then bind with the negatively charged particle faces and form a particulate network. Support for the above mechanism is provided by a series of systematic experiments along with data from dynamic light scattering (DLS) and small-angle neutron scattering (SANS).

In closing this section, it is worth reiterating that the three components of the present PR fluids (i.e., laponite, PAG, and PF127) are all commercially available and relatively inexpensive. Thus, our results can be replicated easily by other researchers who have an interest in PR fluids. Second, it is worth pointing out the analogy between our PR system with existing electrorheological (ER) fluids[24] and magnetorheological (MR) fluids.[25] ER and MR fluids are those whose rheology can be modulated by external electric or magnetic fields, respectively. Both types of fluids are dispersions of micron-sized particles in a solvent; in the "off" state, the particles are unconnected and the sample is of low viscosity, whereas when the field is switched on, the particles get connected into a network and the sample develops a yield stress.[24,25] The same mechanism underlies the behavior of our PR system as well. To our knowledge this is the first demonstration of a nanoparticle-based photorheological fluid.

2. Experimental Section

Materials. Laponite RD was obtained from Southern Clay Products. The nanoparticles are disklike with a diameter of 25 nm and a thickness of 0.92 nm. Pluronic F127 (PF127) was reagent grade and was purchased from Sigma Aldrich. The material is a triblock copolymer of the form PEO−PPO−PEO, where PEO refers to poly(ethylene oxide) and PPO to poly(propylene oxide). The percentages of PEO and PPO are ∼70% and 30%, respectively, and the overall molecular weight is 12 kDa. The PAG, diphenyliodonium-2-carboxylate monohydrate, was purchased from TCI America (purity >98%). Ultrapure deionized water from a Millipore water-purification system was used in preparing samples for rheological characterization, while D_2O (99.95% deuterated, from Cambridge Isotopes) was used for the SANS studies.

Sample Preparation. Dispersions of laponite particles were prepared by adding the particles to water, followed by vortex mixing for 5 min. A Branson 1510 sonicator was then used for 1 h at 40 kHz to fully disperse the particles. Weighted quantities of PF127 were then added to the laponite dispersions, and the mixture was stirred for 1 h using a magnetic stirrer bar. Thereafter, weighted quantities of the PAG were added to the dispersion. Samples were stirred continuously overnight to fully dissolve the PAG and to ensure that the final sample was completely homogeneous.

Sample Response before and after UV Irradiation. Laponite/PF127/PAG samples were irradiated with UV light from a Oriel 200 W mercury arc lamp. A dichroic beam turner with a mirror reflectance range of 280 to 400 nm was used to access the UV range of the emitted light. Samples (5−15 mL) were placed in a

(14) Theng, B. K. G. *The Chemistry of Clay-Organic Reactions*; Wiley: New York, 1974.
(15) van Olphen, H. *An Introduction to Clay Colloid Chemistry*; Wiley: New York, 1977.
(16) Thompson, D. W.; Butterworth, J. T. *J. Colloid Interface Sci.* **1992**, *151*, 236–243.
(17) Dijkstra, M.; Hansen, J. P.; Madden, P. A. *Phys. Rev. Lett.* **1995**, *75*, 2236–2239.
(18) Nelson, A.; Cosgrove, T. *Langmuir* **2005**, *21*, 9176–9182.
(19) Reichmanis, E.; Houlihan, F. M.; Nalamasu, O.; Neenan, T. X. *Chem. Mater.* **1991**, *3*, 394–407.
(20) Dektar, J. L.; Hacker, N. P. *J. Org. Chem.* **1990**, *55*, 639–647.
(21) Gu, H. Y.; Zhang, W. Q.; Feng, K. S.; Neckers, D. C. *J. Org. Chem.* **2000**, *65*, 3484–3488.
(22) Gu, H. Y.; Ren, K. T.; Grinevich, O.; Malpert, J. H.; Neckers, D. C. *J. Org. Chem.* **2001**, *66*, 4161–4164.
(23) Scherrer, R. A.; Beatty, H. R. *J. Org. Chem.* **1980**, *45*, 2127–2131.
(24) Hao, T. *Adv. Mater.* **2001**, *13*, 1847–1857.
(25) Rankin, P. J.; Ginder, J. M.; Klingenberg, D. J. *Curr. Opin. Colloid Interface Sci.* **1998**, *3*, 373–381.

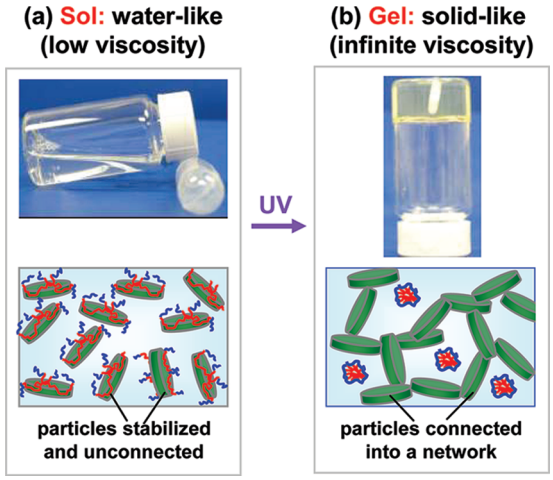

Figure 2. Photogelling of a 3% laponite + 3.6% PF127 + 13 mM PAG sample. Initially (a), the sample is a low-viscosity fluid: the particles are unconnected and stabilized by the adsorbed PF127. Upon UV irradiation (b), the particles assemble into a "house-of-cards" network, causing the fluid to turn into a gel. In this case, the PF127 no longer covers the particle surface; instead it forms discrete micelles in solution. Note that the photogel holds its weight in the inverted vial, and the stirrer bar is trapped in it.

20 mL vial with a quartz cover, and irradiation was done for a specific duration under stirring. Alternately, 1 mL samples were placed in a 3 mL vial with a quartz cover, and irradiation was done without stirring. Irradiated samples did not undergo any changes when stored under ambient conditions, which facilitated subsequent tests using techniques such as rheology and SANS.

Rheological Studies. Steady and dynamic rheological experiments were performed on an AR2000 stress controlled rheometer (TA Instruments, Newark, DE). Samples were run at 25 °C on a cone-and-plate geometry (40-mm diameter, 4° cone angle) or a Couette geometry (rotor of radius 14 mm and height 42 mm, and cup of radius 15 mm). To minimize loading effects on the gel samples, experiments were performed 1 h after loading. Dynamic frequency spectra were obtained in the linear viscoelastic regime of each sample, as determined by dynamic stress-sweep experiments.

Small Angle Neutron Scattering (SANS). SANS measurements were made on the NG-7 (30 m) beamline at NIST in Gaithersburg, MD. Neutrons with a wavelength of 6 Å were selected. Three sample−detector distances of 1, 4, and 13 m were used to probe wave vectors from 0.004 to 0.4 $Å^{-1}$. Samples were studied in 2 mm quartz cells at 25 °C. Scattering spectra were corrected and placed on an absolute scale using calibration standards provided by NIST.

Dynamic Light Scattering (DLS). DLS measurements were made on a Photocor-FC light scattering instrument with a 5 mW laser light source at 633 nm with a scattering angle of 90°. A logarithmic correlator was used to measure the intensity autocorrelation function, from which the hydrodynamic radius was obtained by analysis using the method of cumulants coupled with the Stokes−Einstein equation.

3. Results and Discussion

Photogelling: Rheological Studies. Our photogelling samples were made by combining laponite, PF127, and PAG in deionized water. Figure 2 shows photographs of a sample of 3% laponite together with 3.6% of PF127 and 13 mM of PAG. Initially (Figure 2a), such dispersions are stable, low-viscosity sols. It is known that PF127 imparts steric stabilization to laponite dispersions: as indicated by the schematic in Figure 2a, the hydrophobic PPO segment of PF127 (shown in red) adsorbs onto the faces of the particles while the hydrophilic PEO segments (shown in blue) stretch out into the water.[18] Addition

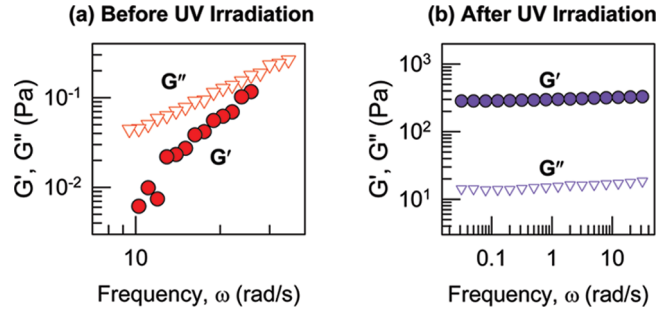

Figure 3. Dynamic rheology of a 1.4% laponite + 1.7% PF127 + 13 mM PAG sample (a) before and (b) after 15 min of UV irradiation. Before UV irradiation, the sample shows a purely viscous response, characteristic of a liquid. After irradiation, the sample response is purely elastic and characteristic of a gel. The gel modulus is ~300 Pa.

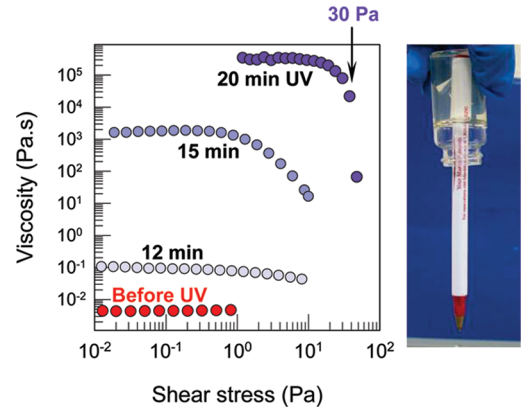

Figure 4. Steady-shear rheology of a 3% laponite + 3.6% PF127 + 13 mM PAG sample before and after UV irradiation for various periods of time. The sample switches from a low-viscosity, Newtonian fluid to a strong gel with progressive irradiation. The final gel has a yield stress of ~30 Pa, which is sufficient to hold the weight of a pen.

of the PAG had no effect on dispersion stability or the sample viscosity: samples remained unchanged for months. The laponite/PF127/PAG sol in Figure 2a was then subjected to UV light, whereupon the PAG was photolyzed to benzoic acid and iodobenzene (see scheme in Figure 1c).[21,22] Figure 2b shows the macroscopic outcome of UV irradiation for 20 min: the low-viscosity sol is transformed into a strong gel that holds its weight in the inverted vial. Note from the photograph that the stirrer bar remains trapped in the gel.

To quantify the light-induced changes in rheological properties, we first turned to dynamic rheology. Figure 3 shows typical dynamic rheological data (elastic modulus G' and viscous modulus G'' as functions of frequency ω) for a sample before and after UV irradiation. The sample contains 1.4% laponite, 1.7% PF127, and 13 mM PAG. Before UV irradiation, the response of the sample is characteristic of a purely viscous sol: $G'' > G'$, with both G' and G'' being strong functions of frequency.[26] On the other hand, after 15 min of UV irradiation, the sample has been drastically altered: its response is now purely elastic, as is characteristic of a permanent gel. That is, $G' \gg G''$, with both moduli being independent of frequency.[26] The gel modulus G_0 is the value of the elastic modulus G' as the frequency $\omega \rightarrow 0$ and is ~300 Pa. Thus, a light-induced sol−gel transition is confirmed by the dynamic rheological data.

(26) Macosko, C. W. *Rheology: Principles, measurements and applications*; VCH Publishers: New York, 1994.

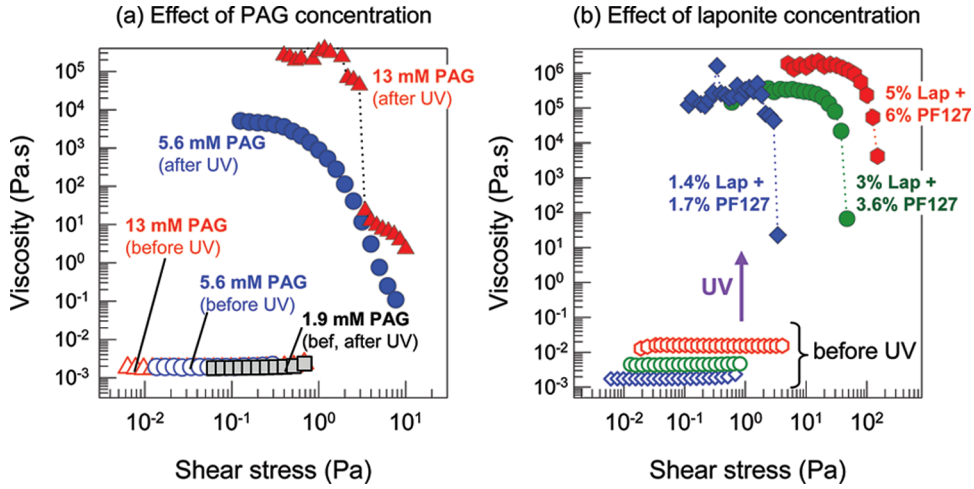

Figure 5. (a) Effect of PAG concentration on photogelling. Steady-shear data are shown for samples containing 1.4% laponite + 1.7% PF127 + various amounts of PAG before and after 15 min of UV irradiation. (b) Effect of laponite concentration on photogelling. Steady-shear data before and after UV irradiation for 20 min are shown for samples containing 13 mM PAG with various amounts of laponite + PF127. In both cases, data before UV are shown using unfilled symbols, and data after UV with filled symbols.

Figure 4 shows steady-shear rheological data (viscosity vs shear stress) on a photogelling sample. The data also simultaneously illustrate the time-dependence of the light-induced changes. The sample is 3% laponite + 3.6% PF127 + 13 mM PAG (same as that in Figure 2). Before UV irradiation, the sample is a Newtonian liquid with a low viscosity of 4.4 mPa·s (i.e., ~4 times the viscosity of the solvent, water). After 12 min of irradiation, the zero-shear viscosity η_0 (i.e., the viscosity at low shear-stresses or shear-rates) is increased by a factor of ~20 and the sample shows weak shear-thinning. By the 15 min mark, η_0 has been further increased by another 4 orders of magnitude and the sample becomes strongly shear-thinning. After 20 min, η_0 is essentially infinite at low stresses (i.e., the sample is a gel). The sample has a finite yield stress of ~30 Pa: this is the value of the stress at which the viscosity begins to plummet (see arrow). As shown by the photograph, this yield stress is high enough to support the weight of an embedded pen. We should point out here that the rate of photogelling is limited by the rate of absorption of UV light by the sample (PAG photolysis itself occurs in nanoseconds[19]). Thus, photogelling can be hastened by using higher intensity lamps and/or smaller sample volumes (path lengths).[12,13]

We now describe how the extent of photogelling varies with sample composition. First, Figure 5a shows the effect of PAG concentration. As stated earlier, addition of PAG has no influence on the initial viscosity of laponite + PF127 dispersions; thus, the initial viscosities for 1.9, 5.6, and 13 mM PAG overlap (the initial pH in all cases is ~9.6−9.8). However, the amount of PAG does influence the photogelling. If the PAG concentration is very low (1.9 mM), no light-induced viscosity increase is seen and the data before and after irradiation are identical. For moderate amounts of PAG (5.6 mM), the viscosity increases appreciably upon exposure to light. Finally, with sufficiently high PAG amounts (13 mM), the full extent of photogelling occurs. Further addition of PAG beyond 13 mM did not increase the yield stress of the photogel. Note that the higher the PAG concentration, the lower the pH after irradiation: the pH values were 8.5, 7.8, and 7.4, respectively, for 1.9, 5.6, and 13 mM PAG. The light-induced reduction in pH is one key aspect in the mechanism for photogelling, as will be discussed later.

The strength of the photogel can also be modulated by varying the concentration of laponite particles. Figure 5b shows rheology data before and after UV irradiation for three samples, all containing 13 mM of PAG. The laponite concentration is varied from 1.4% to 3% to 5%, and the PF127 concentration is proportionately increased to keep the particles stable initially. With increasing laponite, the initial viscosity of the sample is marginally higher, while the sample response remains Newtonian in all cases. All three samples are gelled by exposure to UV, with the yield stress of the photogel increasing from 3 Pa for the 1.4% sample to 30 Pa for the 3% sample and finally to 100 Pa for the 5% laponite sample.

Photogelling: SANS Studies. The results so far provide clear experimental evidence for photogelling in laponite/PF127/PAG samples. We can attribute this effect to a transition from unconnected laponite particles before irradiation to a 3-D network of the same particles after irradiation, as shown by Figure 2. To substantiate this mechanism, we first resorted to SANS. Samples were made in D_2O to attain the required contrast between the structures of interest and the solvent: these samples were visually and rheologically identical to those in H_2O. Figure 6 shows SANS spectra (I vs q) for 1.4% Laponite + 1.7% PF127 dispersions at three different PAG concentrations: 1.9, 5.6, and 13 mM. Data are provided both before and after UV irradiation. Before irradiation, the data are identical at the three PAG concentrations, which is consistent with the rheological data in Figure 5a. In all cases, the scattering intensity shows a plateau at low q, which suggests that there is no large-scale particle aggregation; i.e., the laponite particles are initially well-dispersed. After irradiation, a significant rise in low-q scattering intensity is seen for the samples that photogel (5.6 and 13 mM PAG). In comparison, there is no increase in low-q scattering intensity for the 1.9 mM PAG sample that does not photogel as per Figure 5a. A rise in low-q intensity signifies growth of large structures and/or attractive interparticle interactions.[27]

(27) *Neutron, X-Ray and Light Scattering: Introduction to an Investigative Tool for Colloidal and Polymeric Systems*; Zemb, T., Lindner, P., Eds.; Elsevier: Amsterdam, 1991.

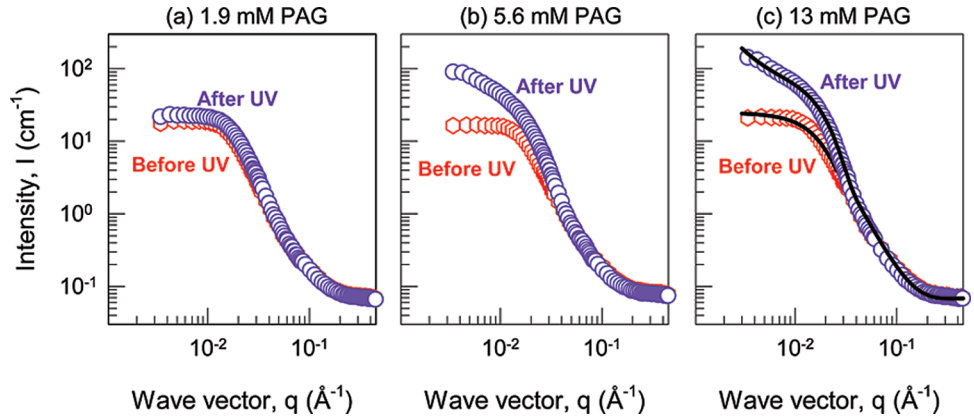

Figure 6. SANS scattering spectra (intensity I vs wave-vector q) for samples containing 1.4% laponite + 1.7% PF127 and with three different PAG concentrations. Data before UV irradiation are shown as red symbols and that after 15 min of UV irradiation are shown as violet symbols. For the 13 mM PAG sample, the data before and after UV are fit to models as described in the text, and the model fits are shown as solid lines.

Thus, we can directly infer a change from unconnected to connected particles even without the benefit of insights from modeling.

We have also fit models to the SANS data in Figure 6c. Details of the models used are provided in the Supporting Information. For the initial system of stabilized particles, we model the laponite covered by PF127 as core−shell disks, as has been done by Nelson and Cosgrove.[18] The laponite core is fixed to have a diameter of 25 nm and a thickness of 0.9 nm, while the dimensions of the PF127 shell are obtained from model fitting: shell thicknesses of 1.5 nm over the particle face and 0.5 nm over the particle edge are obtained. All these dimensions are consistent with previous reports.[18,28] In addition to the stabilized particles, the presence of discrete micelles of PF127 in the solution must also be included in the model.[18] Again, consistent with the literature, these micelles are considered to be core−shell spheres with a PPO core and a PEO shell.[29] From the model fit,[30] a core diameter of 1.6 nm and a shell thickness of 0.4 nm are estimated for these micelles. Importantly, no structure factor needs to be included to model the system before UV irradiation; our model only takes into account the form factors of the PF127-covered laponite particles and of the free PF127 micelles. The ability to model the data without a structure factor confirms our assumption that the particles are discrete and experience no significant long-range interactions.[27]

Next, we consider the same system after UV irradiation, i.e., after it has undergone photogelling. In this case, the particles are expected to be connected into a volume-filling network. We therefore include a fractal structure factor[30,31] in the model for the laponite particles, in addition to the form factors from above (i.e., core−shell disks for the particles, core−shell spheres for the PF127 molecules/micelles). From the model fit, we obtain a fractal dimension of 2 for the laponite gel, consistent with the findings of Pignon et al.[32] With regard to the particles, the shell dimensions are reduced to near zero, indicating that the particles are mostly just the laponite core; i.e., the PF127 is no longer adsorbed on the particles. The desorbed PF127 forms micelles in solution having a core diameter of 12 nm and a shell thickness of 2 nm. The larger dimensions for the micelles following UV irradiation indicate that they are composed of numerous PF127 chains; also, they likely encapsulate the hydrophobic byproduct of the photolysis (iodobenzene) in their core. All in all, SANS modeling provides numerous insights which are used below in formulating a detailed photogelling mechanism.

Photogelling: Mechanism. We now put forth a mechanism for photogelling, illustrated in Figure 7, starting from molecular events and correlating these to structural transitions. Initially (before irradiation), the laponite/PF127/PAG sample is a sol, with the particles stabilized and unconnected. Upon UV irradiation, the sample is transformed into a gel, with the laponite particles connected into a network. How does UV light transform the sol into a gel? The only light-sensitive component of the system is the PAG, and PAG photolysis gives rise to benzoic acid and iodobenzene (Figure 1c).[21,22] An obvious question then is whether addition of benzoic acid and iodobenzene to a laponite/PF127 sol can convert it into a gel. We have tested this, and the results are schematically captured in Figure 8a. As an example, consider a stable sol of 1.4% laponite and 1.7% PF127. If benzoic acid *alone* or iodobenzene *alone* was added to this sample, no gelling occurred regardless of the concentration of the additives. On the other hand, if 13 mM of benzoic acid and iodobenzene *were both added*, gelling did occur; this indicates that each component of PAG photolysis has a crucial role to play.

A key related insight into laponite particles is that, as pH drops below 9, laponite particle edges acquire a positive charge,[15,16] which allows their interactions with negatively charged faces and leads to a network of particles. Such a network is called a "house-of-cards" gel.[14−17] In our system, we believe the photolysis products of the PAG work in tandem to drive a transition from a sol to a house-of-cards gel. In particular, *the iodobezene drives the PF127 molecules off the laponite particles, while the benzoic acid lowers the solution pH from ∼10 to ∼8 and thereby makes the laponite edges positively charged*. Both these events are depicted in Figure 7. Note that iodobenzene is hydrophobic, and while a few molecules may adsorb on the laponite, most will get solubilized in PF127 micelles (also depicted in Figure 7). In either case, PF127 that was previously adsorbed will be driven into solution in the form of micelles. The absence of the steric barrier provided by PF127

(28) Nelson, A.; Cosgrove, T. *Langmuir* **2004**, *20*, 2298–2304.
(29) Wanka, G.; Hoffmann, H.; Ulbricht, W. *Macromolecules* **1994**, *27*, 4145–4159.
(30) Pedersen, J. S. *Adv. Colloid Interface Sci.* **1997**, *70*, 171–210.
(31) Teixeira, J. *J. Appl. Crystallogr.* **1988**, *21*, 781–785.
(32) Pignon, F.; Magnin, A.; Piau, J. M.; Cabane, B.; Lindner, P.; Diat, O. *Phys. Rev. E* **1997**, *56*, 3281–3289.

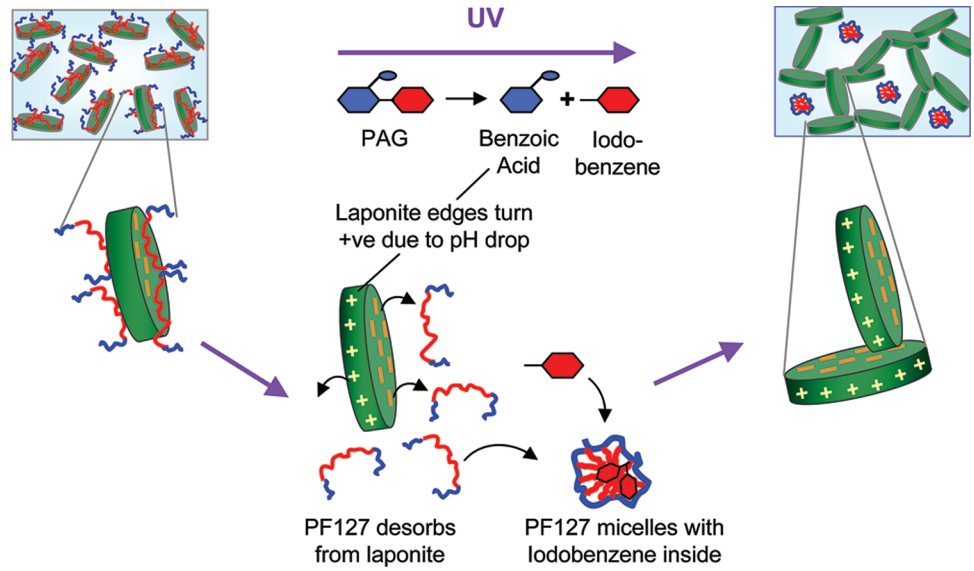

Figure 7. Mechanism for photogelling. Initially, laponite disks are stabilized by PF127, with the hydrophobic PPO portion (red segment) of PF127 adsorbed on the particles and the hydrophilic PEO portions (blue) extending into water. Upon UV irradiation, the PAG splits into benzoic acid and iodobenzene. The PF127 desorbs from the laponite and forms micelles in solution, taking up the hydrophobic iodobenzene. The lowering of pH by the benzoic acid causes the particle edges to turn positive. In turn, the particles assemble into a network due to interactions between the positive edges and the negative faces.

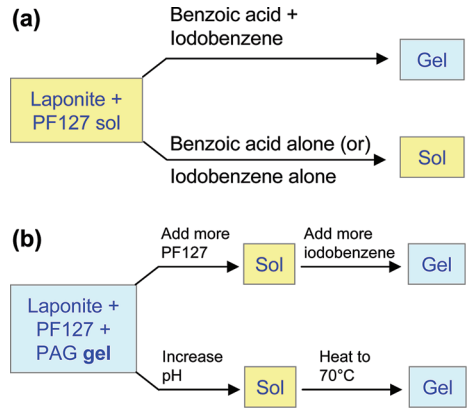

Figure 8. Schematics of experiments that give insight into the photogelling mechanism. (a) A sol of laponite+PF127 can be gelled if both iodobenzene and benzoic acid are added, but not if only one of the two are added. (b) A gel of laponite+PF127+PAG can be liquefied (ungelled) by either adding more PF127 or by increasing the pH. The former can be gelled again by adding more iodobenzene. The sols are also temperature sensitive and can be gelled by heating to 70 °C.

will allow the negatively charged laponite faces to interact with the positively charged laponite edges and form a house-of-cards gel,[14−17] as shown in the right-hand panel of Figure 7.

Many disparate pieces of evidence have been used to put together the above mechanism. Some have been mentioned earlier: e.g., the drop in sample pH upon UV irradiation was discussed in the context of Figure 5a; also, the parameters from SANS modeling are consistent with the desorption of PF127 from the laponite particles upon UV irradiation. Further support is provided by a study on iodobenzene addition to an aqueous solution containing PF127. While iodobenzene was not soluble in pure water, it did get solubilized in the presence of PF127. In fact, we found that *iodobenzene induced PF127 micelles*: e.g., a 1.7% PF127 solution gave no indication of micelles by DLS, whereas, upon addition of 13 mM iodobenzene, micelles with a diameter of 28 nm were measured in the solution by DLS. This result implies that the PF127 adsorbed on laponite is likely to desorb and form micelles when iodobenzene is added. Again, note that desorption of PF127 from the particles is not sufficient for gelling: the pH must also be reduced to alter the charge on the particle edges. Such a pH reduction can be induced by benzoic acid, which explains the results of Figure 8a. Experimentally, we have found that benzoic acid is not unique in this context: any other acid like HCl could also be used to lower the pH and thereby cause gelation.

Finally, we should mention that a photogelled laponite/PF127/PAG sample can be ungelled (converted back to a low-viscosity fluid) in a couple of different ways (Figure 8b), both of which are consistent with the above mechanism. First, adding more PF127 to a photogel will ungel it, and if iodobenzene is subsequently added, the solution can be gelled again. This result means that if PF127 is replenished on the particle surface, there will be no gel; if the new PF127 is driven off the particles by fresh iodobenzene, the gel will form again. Second, the photogel can be ungelled by increasing the pH back to ∼10, e.g., by adding NaOH or other bases. This result confirms the key role of pH in ensuring positively charged particle edges, which are needed for gelation.[15,16] Interestingly, the same system is also responsive to temperature: the sol generated by an increase in pH can also be gelled by heating the sample to >70 °C (Figure 8b). The temperature response is not fully understood and is being investigated in more detail. Nevertheless, it is striking that a single complex fluid can show sensitivity to a variety of commonly studied stimuli: light, pH, and temperature.

4. Conclusions

We have demonstrated UV-induced photogelling in laponite/PF127/PAG mixtures. Initially, the PF127 is adsorbed on the faces of laponite particles, which sterically stabilizes them from aggregation. Upon UV irradiation, the PAG is photolyzed into benzoic acid and iodobenzene. The formation of benzoic acid drops the solution pH from 10 to 8, which in turn makes the particle edges positively charged. The iodobezene, on the other hand, drives the PF127 off the particle faces and into solution where the PF127 forms micelles with iodobenzene in its cores.

This frees up the particle edges (+) and faces (−) for interaction, which drives the assembly of a house-of-cards network. The water-like sol is thus transformed into a stiff elastic gel having a sufficient yield stress to hold its own weight or the weight of small embedded objects.

Acknowledgment. This work was partially funded by a CAREER award from NSF-CBET. We acknowledge NIST NCNR for enabling the SANS experiments performed as part of this work.

Supporting Information Available: Additional details on the SANS modeling in Figure 6. This material is available free of charge via the Internet at http://pubs.acs.org.

JA9008584

Supporting Information for

Photogelling Colloidal Dispersions Based on Light-Activated Assembly of Nanoparticles

Kunshan Sun, Rakesh Kumar, Daniel E. Falvey, and Srinivasa R. Raghavan*

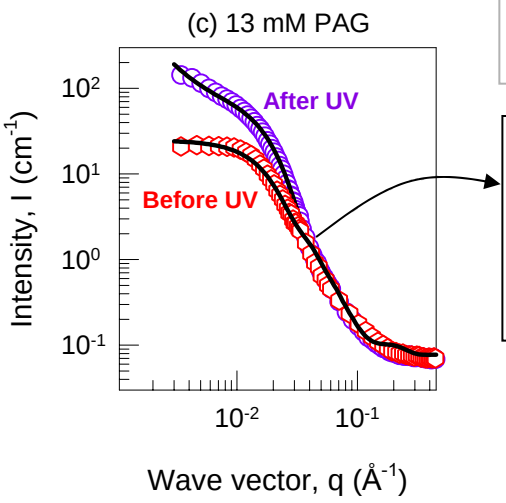

Before UV

Before UV: data modeled as:
Form Factor for Core-Shell Disks = Laponite covered with PF127 = $P_1(q)$ +
Form Factor for Core-Shell Spheres = PF127 micelles = $P_2(q)$
Structure Factor $S(q)$ = 1, i.e., no interactions

Form Factor for Core-Shell Disks: see Nelson & Cosgrove (Ref. 18)
Core of the disk = laponite (25 nm diameter, 0.9 nm radius)
Shell of the disk = PF127

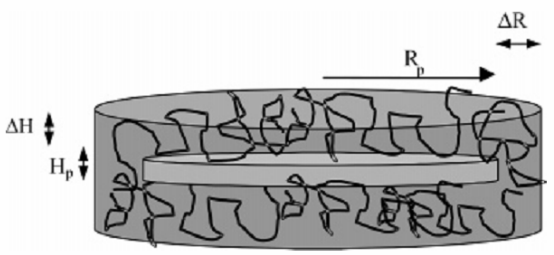

schematic from Nelson & Cosgrove[18]

Form factor for core-shell disks:

$$P_1(q) = \frac{1}{V_p}\int_0^{\pi/2} \sin\theta d\theta \left\{ V_1(\rho_1 - \rho_{solv}) \frac{\sin\left[q(H_p + 2\Delta H)(\cos\theta)/2\right]}{q(H_p + 2\Delta H)(\cos\theta)/2} \frac{2J_1\left[q(R_p + \Delta R)\sin\theta\right]}{q(R_p + \Delta R)\sin\theta} + V_p(\rho_p - \rho_1) \frac{\sin\left[qH_p(\cos\theta)/2\right]}{qH_p(\cos\theta)/2} \frac{2J_1\left[qR_p\sin\theta\right]}{qR_p\sin\theta} \right\}^2$$

where $J_1(x) = \frac{\sin x - x\cos x}{x^2}$

Parameters (Core):
V_p = volume of core
R_p = radius of core = 25 nm
H_p = thickness of core = 0.9 nm
ρ_p = scattering length density of the core

Parameters (Shell):
ΔR = shell thickness on the edge
ΔH = shell thickness on the face
ρ_1 = scattering length density of the shell

Parameters (Other):
V_1 = total volume of particle core and shell
ρ_{solv} = scattering length density of the solvent

Form Factor for Core-Shell Spheres: see Pedersen (Ref. 30)

$$P_2(q) = \frac{1}{\langle V_m \rangle} \int_0^{r=\infty} f(r) F^2(qr) dr \quad \text{where} \quad F(qr) = p^3(\rho_c - \rho_s) V_m \frac{3J_1(qpr)}{qpr} + (\rho_s - \rho_{solv}) V_m \frac{3J_1(qr)}{qr}$$

Parameters:

r = overall radius (core+shell)

pr = radius of core

V_m = volume of the sphere; $\langle V_m \rangle$ = average volume

ρ_c = scattering length density of the core

ρ_s = scattering length density of the shell

ρ_{solv} = scattering length density of the solvent

$f(r)$ = Schulz distribution for the polydispersity of the sphere

Key Parameters	**Values with error bars**
Shell thickness (edge) (nm)	0.5 ± 0.016
Shell thickness (face) (nm)	1.5 ± 0.002
Micelle core diameter (nm)	1.6 ± 0.013
Micelle shell thickness (nm)	0.4 ± 0.008

After UV

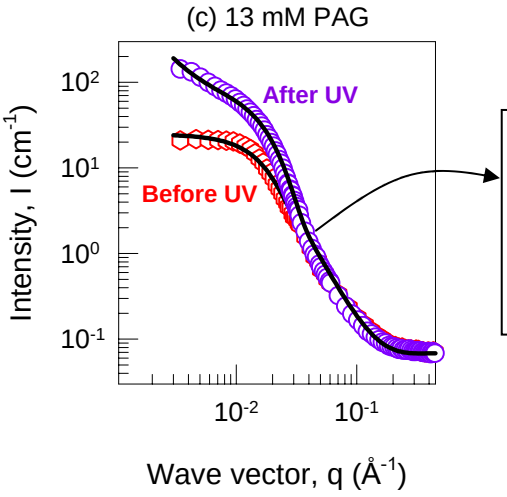

After UV data modeled as:

Form Factor for Core-Shell Disks = Laponite covered with PF127 = $P_1(q)$ +

Form Factor for Core-Shell Spheres = PF127 micelles = $P_2(q)$

Fractal Structure Factor for Disk Network = $S_1(q)$

Fractal Structure Factor for Disk Network : see Teixeira (Ref. 31)

$$S_1(q) = 1 + \frac{D}{r_0^D}\int_0^\infty l^{D-1}\exp\left(-l/\xi\right)\frac{\sin(ql)}{ql}dl$$

Parameters:

D = fractal dimension

r_0 = effective radius of the particles

ξ = correlation length

l = distance between particles

Key Parameters	Values with error bars
Shell thickness (edge) (nm)	0.0 ± 0.015
Shell thickness (face) (nm)	0.3 ± 0.009
Micelle core diameter (nm)	12 ± 0.056
Micelle shell thickness (nm)	2 ± 0.015
Fractal dimension	2 ± 0.02